ELSEVIER

Epilepsy Research 48 (2002) 43–56

Epilepsy Research

www.elsevier.com/locate/epilepsyres

# Heightened seizure severity in somatostatin knockout mice

Paul S. Buckmaster [a,*], Veronica Otero-Corchón [b], Marcelo Rubinstein [c], Malcolm J. Low [b]

[a] *Departments of Comparative Medicine and Neurology & Neurological Sciences, Stanford University, 300 Pasteur Drive, R102 Edwards Building, MC 5330, Stanford, CA 94305-5330, USA*

[b] *Vollum Institute, Oregon Health & Science University, Portland, OR 97201, USA*

[c] *Instituto de Investigaciones en Ingeniería Genética y Biologia Molecular, CONICET, Departmento de Ciencias Biologicas, FCEyN, University of Buenos Aires, Buenos Aires, Argentina*

Received 9 July 2001; received in revised form 21 September 2001; accepted 25 September 2001

**Abstract**

Patients and experimental models of temporal lobe epilepsy display loss of somatostatinergic neurons in the dentate gyrus. To determine if loss of the peptide somatostatin contributes to epileptic seizures we examined kainate-evoked seizures and kindling in somatostatin knockout mice. Somatostatin knockout mice were not observed to experience spontaneous seizures. Timm staining, acetylcholinesterase histochemistry, and immunocytochemistry for NPY, calbindin, calretinin, and parvalbumin revealed no compensatory changes or developmental abnormalities in the dentate gyrus of somatostatin knockout mice. Optical fractionator counting of Nissl-stained hilar neurons showed similar numbers of neurons in wild type and somatostatin knockout mice. Mice were treated systemically with kainic acid to evoke limbic seizures. Somatostatin knockout mice tended to have a shorter average latency to stage 5 seizures, their average maximal behavioral seizure score was higher, and they tended to be more likely to die than controls. In response to kindling by daily electrical stimulation of the perforant path, to more specifically challenge the dentate gyrus, mean afterdischarge duration in somatostatin knockout mice was slightly longer, but the number of treatments to five stage 4–5 seizures was similar to controls. Although we cannot exclude the possibility of undetected compensatory mechanisms in somatostatin knockout mice, these findings suggest that somatostatin may be mildly anticonvulsant, but its loss alone is unlikely to account for seizures in temporal lobe epilepsy. 

*Keywords:* Dentate gyrus; Hilus; Kindling; Kainic acid; Temporal lobe epilepsy

## 1. Introduction

Temporal lobe epilepsy is the most common form of epilepsy in adults and one of the most difficult types to treat (Engel et al., 1997). In patients and experimental models of temporal lobe epilepsy, the loss of hilar somatostatinergic

* Corresponding author. Tel.: +1-650-498-4774; fax: +1-650-498-6259.

*E-mail address:* psb@stanford.edu (P.S. Buckmaster).

0920-1211/02/$ - see front matter 
PII: S0920-1211(01)00318-7

interneurons is the best documented and most consistent interneuron deficit. It was reported first by de Lanerolle et al. (1989), who proposed that the loss of hilar somatostatinergic interneurons reduces functional inhibition of granule cells in the dentate gyrus and lowers seizure threshold. These findings were extended with neurochemical and in situ hybridization data (Robbins et al., 1991). Mathern et al. (1995) found that in the anterior hippocampus of patients with temporal lobe epilepsy, the number of hilar somatostatin-immunoreactive interneurons is reduced to less than 20% of control values.

Laboratory animal models of temporal lobe epilepsy provide additional support for a correlation between epilepsy and the loss of hilar somatostatin-immunoreactive interneurons. Somatostatinergic interneurons are the most abundant interneuron type in the hilus of the dentate gyrus. In rats, they account for 20% of all hilar neurons and 50% of GABAergic hilar neurons (Houser and Esclapez, 1996; Buckmaster and Dudek, 1997; Buckmaster and Jongen-Rêlo, 1999). In rats there are significantly fewer hilar somatostatin-immunoreactive interneurons compared with controls after pilocarpine treatment (Houser and Esclapez, 1996), prolonged perforant path stimulation (Freund et al., 1991; Sloviter, 1987), tetanus toxin induced seizures (Mitchell et al., 1995), ischemia (Johansen et al., 1987), head trauma (Lowenstein et al., 1992), kainate treatment (Magloczky et al., 1993; Sperk et al., 1992) and status epilepticus induced by rapid kindling (Schwarzer et al., 1995). Kainate-induced epileptic rats, for example, have on average 40–50% fewer hilar somatostatin-immunoreactive interneurons relative to controls (Buckmaster and Dudek, 1997), and hilar somatostatin-immunoreactive interneurons account for 83% of the total loss of GABAergic neurons in the dentate gyrus (Buckmaster and Jongen-Rêlo, 1999).

Thus, human studies and experimental models provide evidence for a correlation between epilepsy and the loss of hilar somatostatinergic interneurons. Somatostatin has been reported to have anticonvulsant effects (Vezzani et al., 1991; Monno et al., 1993; Tallent and Siggins, 1999) and proconvulsive effects (Havlicek and Friesen, 1979; Higuchi et al., 1983). It is unclear whether the loss of hilar somatostatinergic neurons causes hyperexcitability and thereby leads to seizures. And if somatostatinergic neuron loss contributes to seizure genesis, it is unclear whether the mechanism involves the loss of the peptide somatostatin or the loss of other neurotransmitters expressed by these neurons—e.g. GABA (Somogyi et al., 1984; Kosaka et al., 1988; Esclapez and Houser, 1995) and neuropeptide Y (Chan-Palay, 1987; Köhler et al., 1987; Deller and Leranth, 1990). The present study addresses this question by comparing kainate-induced seizures and kindling in somatostatin knockout and wild type mice to determine if loss of the peptide somatostatin contributes to seizure severity.

## 2. Methods

### 2.1. Animals

The adult ($\geq 3$ months old) homozygous somatostatin-deficient and wild type mice used in these experiments were described previously (Low et al., 2001). Briefly, a mutated *Smst* gene allele with deletion of promoter sequences and the first coding exon was generated by homologous recombination in embryonic stem cells. The somatostatin null allele contains a *neo* resistance cassette, but it does not have an expressed reporter gene. Germline chimeric mice were derived by injection of C57BL/6J blastocysts with correctly targeted E14 embryonic stem cells derived from substrain 129P2/Ola mice. $F_1$ heterozygous mice were obtained by mating chimeric males to C57BL/6J females. Subsequently, $F_2$ (C57, 129) mice were obtained by mating $F_1$ males and females, and the three expected somatostatin genotypes were obtained in normal Mendelian proportions. To reduce genetic background variability that is inherent in the original $F_2$ (C57, 129) mutant strain, the somatostatin null allele was backcrossed for five successive generations onto the C57BL/6J inbred strain to produce $N_5$ incipient-congenic mice. Litters of $N_5$ heterozygous mating pairs were genotyped at weaning using genomic DNA prepared from the distal 0.5 cm of tail and a sensitive PCR-based screen.

Somatostatin knockout and wild type mice were healthy and did not display spontaneous seizures. Somatostatin knockout mice were never observed to have behavioral seizures during the following treatments: tail suspension, locomotor activity testing during mid-light and mid-dark cycles ($>1$ h periods of observation), acoustic startle testing (observed 1 h following test), brain stem auditory evoked response testing, restraint for serial tail bleeds (observed 80 min), and 30 min restraint without additional handling (observed up to 6 h following test). During kindling treatments, evoked afterdischarges occurred, but no spontaneous seizures were observed.

### 2.2. Anatomy

To confirm that the mice had been genotyped correctly and to screen knockout mice for developmental abnormalities in the dentate gyrus, they were prepared for anatomical examination of the hippocampus. All of the anatomical comparisons were made with naive wild type and somatostatin knockout mice, except NPY-immunocytochemistry which was used to examine naive and kindled mice. Mice were killed by pentobarbital overdose (100 mg/kg, i.p.) and perfused through the ascending aorta at 15 ml/min for 2 min with 0.9% NaCl, 10 min with 0.37% buffered sodium sulfide, and 30 min with 4% paraformaldehyde and 0.5% glutaraldehyde in 0.1 M phosphate buffer (PB, pH 7.4) at 4 °C. The brain was removed and post-fixed in the same fixative for 12–18 h at 4 °C and then cryoprotected in 30% sucrose in PB. The hippocampus was isolated, straightened, and frozen. A sliding microtome (Jung Histoslide 2000R) set at 30 μm, was used to prepare transverse sections, cut perpendicular to the septotemporal axis, of the entire hippocampus. Two 1/8 series of sections were used for Nissl or Timm staining. The remaining sections were stored at $-80$ °C in 30% ethylene glycol and 25% glycerol in PB until simultaneous immunoprocessing of tissue from all of the mice.

One 1/8 series of sections was stained with thionin. The optical fractionator method was used to estimate the number of Nissl stained hilar neurons, as described previously (West et al., 1991; Buckmaster and Jongen-Rêlo, 1999). Briefly, sections were examined with a microscope equipped with a $100\times$ objective (Zeiss), motorized stage (Ludl Electronic Products), Lucivid (MicroBrightField), and Stereo Investigator software (MicroBrightField). The investigator was blind to the subjects' experimental group. Total section thickness was used for dissector height, and only neuronal 'caps' (i.e. neuronal nuclei that were not cut at the top of section) were counted. This procedure facilitates estimating cell numbers in thinly sectioned tissue, but it underestimates the actual number of cells. There would be no effect on the relative values between groups, because all tissue was processed and analyzed identically. Counting frames ($40\times 40$ μm) were spaced randomly and systematically at intervals of $100\times 100$ μm, so that an average of 16% of the total area of the hilus was sampled. The hilus was defined by its border with the granule cell layer and by straight lines drawn from the tips of the granule cell layer to the proximal tip of the CA3 pyramidal cell layer. The average number of caps counted per dentate gyrus was 295.

Another 1/8 series of sections was processed for Timm staining using a protocol similar to that described previously (Buckmaster and Dudek, 1997). Briefly, slide-mounted sections developed in 150 ml 50% gum arabic, 25 ml 2 M citrate buffer, 75 ml 0.5 M hydroquinone, and 1.25 ml of 19% silver nitrate for 60 min in darkness. Then they were rinsed, counterstained with thionin, dehydrated, and coverslipped.

Additional 1/8 series of sections were processed for somatostatin- or neuropeptide Y (NPY)-immunoreactivity using a previously described protocol (Buckmaster and Dudek, 1997). Briefly, free-floating sections were exposed to 1% $H_2O_2$ for 1 h, 1% sodium borohydride for 1 h, and a blocking solution consisting of 3% goat serum (GS), 2% bovine serum albumin (BSA), and 0.3% Triton X-100 in 0.05 M Tris-buffered saline (TBS, pH 7.4). Sections incubated in anti-somatostatin serum (1:2500, Peninsula Laboratories) or anti-NPY serum (1:10 000, Peninsula Laboratories) at 4 °C for 40 h. After rinsing, sections were exposed to biotinylated anti-rabbit IgG and then avidin-biotin-horse radish peroxidase (1:500, Vec-

tor Laboratories) diluted in 2% BSA and 0.3% Triton X-100 in TBS. Sections reacted in 0.02% diaminobenzidine, 0.04% ammonium chloride, 0.015% glucose oxidase, and 0.1% β-D-glucose until they reached the desired intensity. Then they were rinsed, mounted on gelatin-coated slides, dried, cleared, and coverslipped.

Somatostatin mRNA was detected by in situ hybridization in 16 μm fresh frozen coronal brain sections using an antisense oligonucleotide probe complementary to mouse somatostatin exon 2 and radiolabeled with [$^{35}$S] as described previously (Rubinstein et al., 1992). After hybridization and washing the slides were exposed to one-sided emulsion film (Biomax MR, Kodak) for 2 days to evaluate the quality of the probe, and finally dipped in emulsion (NTBII, Kodak) 1:1 in distilled water and stored in the dark at 4 °C for 5 days. The emulsion was then developed and the sections counterstained with neutral red, dehydrated for 2 min each in an ethanol series and xylenes, and mounted under coverslips with Permount for darkfield microscopy.

Another set of wild type and somatostatin knockout mice was inspected for anatomical abnormalities using antibodies against calretinin, calbindin, and parvalbumin, and cholinergic circuits were visualized by acetylcholinesterase histochemistry. Adult mice (3 months old) of both genotypes were anesthetized with 2% avertin (150 ml/kg) and transcardially perfused with 0.9% NaCl, followed by 50 ml of ice-cold 4% paraformaldehyde in 0.1 M phosphate buffered saline (PBS, pH 7). The brains were removed, post-fixed overnight at 4 °C, and sectioned coronally at 50 μm using a Vibratome. The immunocytochemistry protocol for calretinin, calbindin, and parvalbumin is similar to that described above, except sections were incubated overnight at 4 °C in anti-calretinin serum (1:2000, Chemicon lot AB149), anti-calbindin serum (1:1000, Sigma, clone CL-300), or anti-parvalbumin serum (1:1000, Sigma, clone PA-235). After the chromogen reaction, sections were counterstained with methyl green, dehydrated, and coverslipped. For acetylcholinesterase staining, sections were incubated for 15 h in 100 ml of 50 mM sodium acetate buffer, pH 5.0, 4.0 mM $CuSO_4$, and 16 mM glycine stock solution (6.8 g sodium acetate, 1 g of copper sulfate crystals, and 1.2 g of glycine in 1 L 50 mM sodium acetate buffer, pH 5) to which had been added 116 mg of *S*-acetylthiocholine iodide and 3.0 mg of ethopropazine. The slides were rinsed with water, developed for 10 min in 1% sodium sulfide (pH 7.5), rinsed, dehydrated, and coverslipped.

### 2.3. Kainate-induced seizures

Kainate administration (25 mg/kg, i.p.) was used to induce seizures in limbic structures (Lothman and Collins, 1981; Nadler, 1981; Sperk, 1994) and compare seizure activity in wild type and somatostatin knockout mice. Behavioral seizures were scored as described previously (Morrison et al., 1996; Liu et al., 1999): 0, no effect; 1, motionless; 2, rigid posture with forelimb and/or tail extension; 3, myoclonic jerks of head and neck; 4, forelimb clonus and partial rearing; 5, forelimb clonus, rearing, and falling; and 6, generalized tonic-clonic convulsions with loss of postural tone.

### 2.4. Kindling

Kindling by daily electrical stimulation of the perforant path was used to challenge the dentate gyrus more specifically than systemic kainate administration. Perforant path stimulation is a more selective method of initiating seizures in the dentate gyrus, where hilar somatostatinergic interneurons reside. Mice were anesthetized with pentobarbital (60 mg/kg, i.p.), placed on a heating pad in a stereotaxic apparatus, and prepared for aseptic surgery. A stimulating (250 μm, bipolar, Rhodes Medical) and recording electrode (insulated stainless steel, 125 μm diameter, Plastics One) were implanted in the perforant path and in the hilus of the dentate gyrus, respectively, at the following stereotaxic coordinates (referenced to bregma): stimulating electrode, 4.0 mm posterior, 3.6 mm lateral; recording electrode, 1.8 mm posterior, 1.4 mm lateral. Electrode depths were adjusted to optimize the amplitude of the granule cell population spike. The evoked responses of the dentate gyrus revealed no obvious abnormalities

(e.g. multiple population spikes) in any of the mice. Ground leads were screwed into the anterior and posterior cranium, and all leads were attached to a microplug (Microtech), which was cemented to the skull with dental acrylic. After surgery, mice were allowed to recover for 1 week before kindling began.

Mice were kindled by daily stimulation of the perforant path with a 1 s stimulus train of 1 ms duration square pulses at 60 Hz while they roamed freely within a cage. Stimulus intensity was determined for each mouse individually. During the first recording session, stimulus intensity was gradually increased to the minimum intensity necessary to evoke an afterdischarge (i.e. the afterdischarge threshold) as monitored by the recording electrode in the dentate gyrus. During the kindling process, if a stimulus failed to evoke an afterdischarge, a new higher-intensity afterdischarge threshold was determined and used for subsequent treatments. Final stimulus intensities were 100–650 μA. Electrographic activity of the dentate gyrus was amplified (AI402 SmartProbes and CyberAmp 380, Axon Instruments), observed on-line (Tektronix), and stored on computer (pCLAMP, Axon Instruments). Afterdischarge duration was measured from the end of the stimulus train to the end of the afterdischarge recorded by the electrode in the dentate gyrus. During the kindling treatments, behavioral seizures were classified according to the criteria of Racine (1972): 0, no effect; 1, facial clonus; 2, head nodding; 3, forelimb clonus; 4, rearing; and 5, rearing and falling. Mice were perfused, as described above, 20 days after their last kindling treatment.

## 3. Results

### 3.1. Anatomy

Thionin staining revealed no abnormalities in the cytoarchitecture of the dentate gyrus of somatostatin knockout mice (Fig. 1A). To determine if hilar neurons that normally would have expressed somatostatin are lost during development in somatostatin knockout mice, the number of thionin-stained hilar neurons was estimated in age-matched male wild type and somatostatin knockout mice. There was no significant difference in the number of thionin-stained hilar neurons per dentate gyrus in wild type and somatostatin knockout mice (Table 1).

To screen the major circuitry of the dentate gyrus for normal development in knockout mice, the Timm stain was used. Wild type and somatostatin knockout mice displayed similar patterns of Timm staining. There is a tri-laminar staining pattern in the molecular layer of the dentate gyrus, where afferents from the entorhinal cortex and ipsilateral associational pathway terminate, and black staining where granule cell axons project through the hilus and into the CA3 field (Fig. 1B).

To confirm the absence of somatostatin expression in the dentate gyrus of knockout mice, immunostaining and in situ hybridization were used. All wild type mice displayed somatostatin-immunoreactive cell bodies in the hilus and an immunoreactive fiber plexus in stratum lacunosum-moleculare of CA1, as described previously (Buckmaster et al., 1994). As expected, there was a lack of somatostatin-immunoreactivity in all knockout mice (Fig. 1C). In situ hybridization using an exon 2 oligonucleotide probe revealed positive cells in the hilus and stratum oriens of wild type but not somatostatin knockout mice (Fig. 2).

NPY is coexpressed with somatostatin in some hilar interneurons (Chan-Palay, 1987; Köhler et al., 1987; Deller and Leranth, 1990). To determine if there were differences in the expression of NPY in somatostatin knockout mice, NPY-immunostained sections from unkindled ($n = 8$) and kindled mice ($n = 24$) were examined (Fig. 3). Wild type and somatostatin knockout mice displayed similar patterns of staining. Before kindling (Fig. 3A), NPY-positive neurons were apparent primarily in the hilus but also in the granule cell layer of the dentate gyrus. Twenty days after the last kindling treatment (Fig. 3B), the NPY-positive fiber plexus in the molecular layer of the dentate gyrus and in stratum lacunosum-moleculare of CA1 was more evident, and additional NPY expression occurred in the hilus and in stratum

lucidum of CA3 where granule cell axons project, as described previously for epileptic tissue (de Lanerolle et al., 1989).

Immunostaining for parvalbumin, calretinin, and calbindin was used to compare other interneuron classes of the dentate gyrus, besides

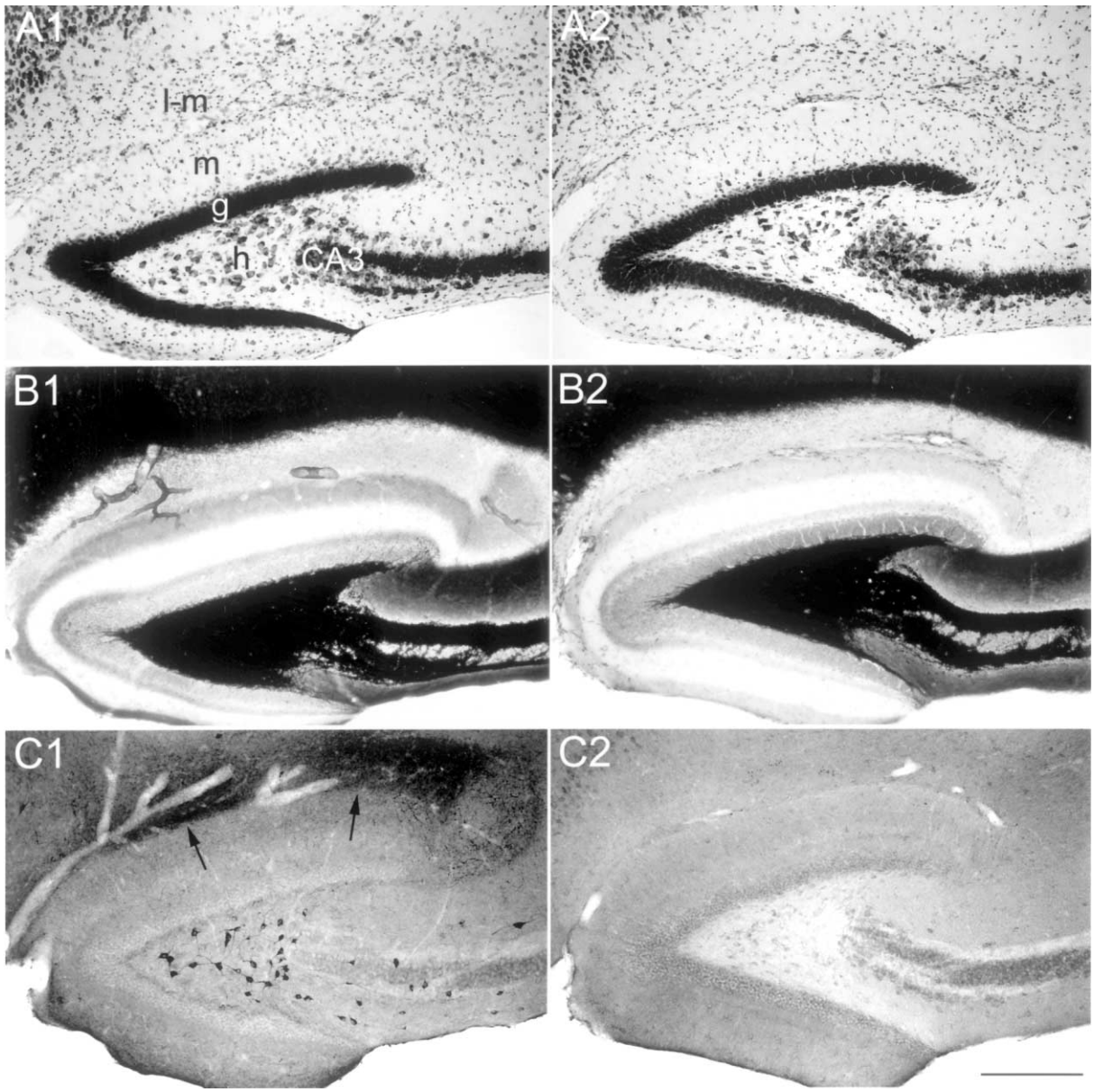


Fig. 1. Nissl staining (A), Timm staining (B), and somatostatin-immunocytochemistry (C) in the dentate gyrus of a wild type (1) and somatostatin knockout mouse (2). Nissl stain reveals normal cytoarchitecture and abundant neurons in the hilus (h) in both mice. Timm stain reveals the normal tri-laminar pattern in the molecular layer (m) and dense, black staining in the hilus and in and around the CA3 pyramidal cell layer (CA3) in both mice. In the wild type mouse, but not in the knockout mouse, somatostatin-immunoreactive neurons are evident in the hilus, and an immunopositive fiber plexus is prominent in stratum lacunosum-moleculare of CA1 (I-m, arrows). Scale bar, 250 μm.

Table 1
Estimated number of hilar neurons per hippocampus in wild type and somatostatin knockout mice

| | Wild type | Somatostatin knockout |
|---|---|---|
| *n* (mice) | 8 | 10 |
| *Hilar neurons* | | |
| Mean | 14 100 | 14 400 |
| S.E.M. | 700 | 600 |
| Range | 12 300–18 700 | 11 300–17 200 |
| C.V. | 0.14 | 0.14 |
| Mean C.E. | 0.10 | 0.06 |

S.E.M., standard error of mean; C.V., coefficient of variation (standard deviation(S.D.)/mean); mean C.E., mean coefficient of error; calculated as described by West et al. (1991).

somatostatinergic interneurons (Fig. 4). There were no obvious differences between wild type and somatostatin knockout mice. Parvalbumin-immunoreactive cell bodies were evident in or near the granule cell layer, and an immunoreactive fiber plexus concentrated in the granule cell layer (Fig. 4A). Granule cell somata and dendrites were calbindin-immunopositive, and a few scattered nonprincipal neurons were also stained (Fig. 4B). Calretinin-immunoreactivity was evident in the inner molecular layer and in some neurons in the hilus (Fig. 4C). This pattern of calretinin staining in the dorsal hippocampus of mice has been described previously (Liu et al., 1996; Blasco-Ibáñez and Freund, 1997; Fujise et al., 1997).

Finally, acetylcholinesterase histochemistry was used to screen for abnormalities in a major subcortical projection to the dentate gyrus. There were no differences between wild type and somatostatin knockout mice (Fig. 5). Both showed the densest fiber staining in the inner molecular layer.

### 3.2. Kainate-induced seizures

In response to kainate (25 mg/kg, i.p.), somatostatin knockout mice ($n = 16$) had slightly more severe seizures than age-matched controls ($n = 9$; Fig. 6). The latency to a stage 5 behavioral score was used to assess seizure susceptibility (Morrison et al., 1996; Liu et al., 1999), because it is the most clearly recognized stage. The average latency to stage 5 seizures was shorter in somatostatin knockout mice ($12.4 \pm 1.7$ min, mean $\pm$ S.E.M.) compared with controls ($22.8 \pm 6.1$ min, $P < 0.07$, $t$-test). The average maximal behavioral seizure score was higher in somatostatin knockout mice ($5.8 \pm 0.1$) than in controls ($4.7 \pm 0.7$, $P < 0.05$, $t$-test). Additionally, somatostatin knockout mice were more likely to die (88%) than controls (56%, $P < 0.08$, $\chi^2$-test).

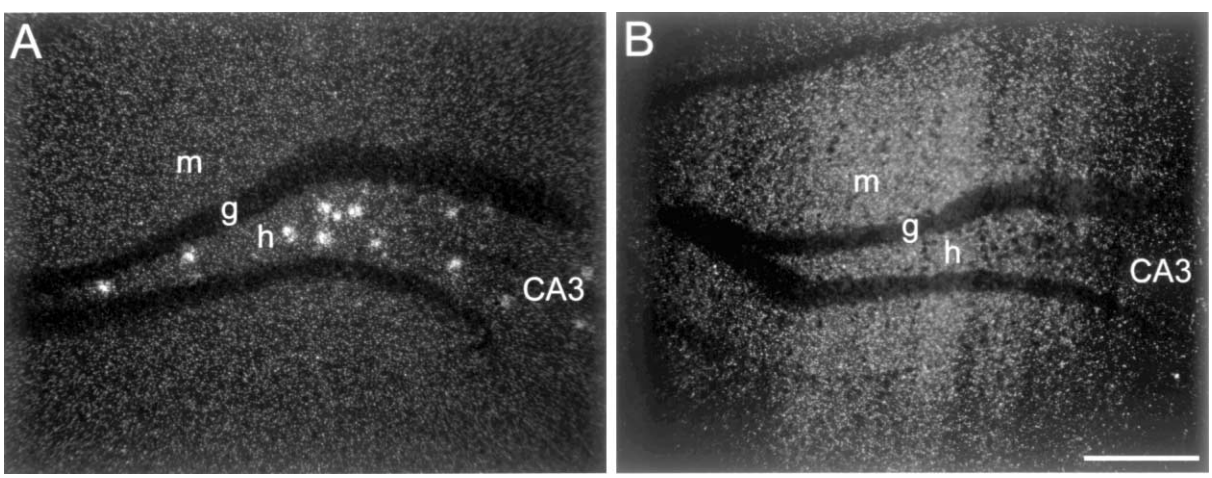


Fig. 2. In situ hybridization for somatostatin mRNA in a wild type (A) and a somatostatin knockout mouse (B). A dense concentration of silver grains over individual somatostatin interneurons is evident in the hilus (h) of the wild type but not the knockout mouse. g, Granule cell layer; m, molecular layer; CA3, CA3 pyramidal cell layer. Scale bar, 250 μm.

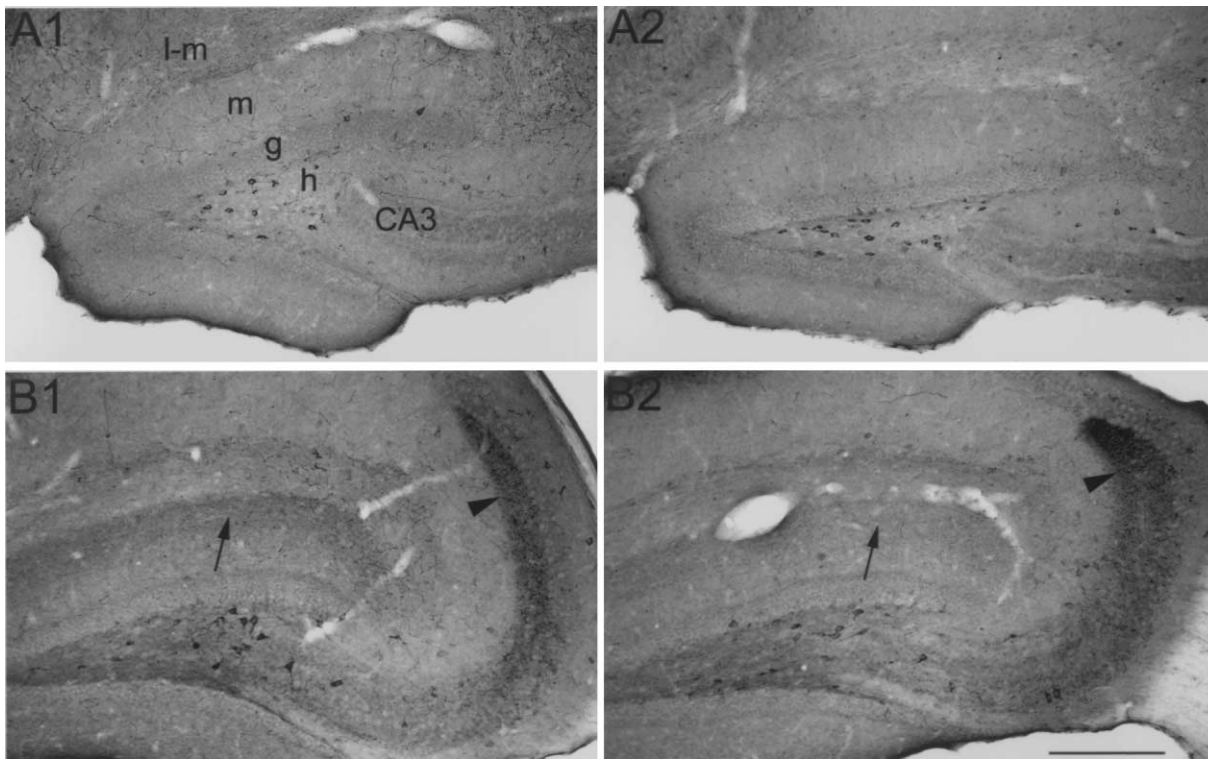


Fig. 3. Similar NPY-immunoreactivity in the dentate gyrus of wild type and somatostatin knockout mice. A1 is from a naive wild type mouse; A2 is from a naive somatostatin knockout mouse. In both mice, NPY-positive cell bodies are evident primarily in the hilus (h), but also in the granule cell layer (g) of the dentate gyrus. B1 is from a kindled wild type mouse; B2 is from a kindled somatostatin knockout mouse. In both kindled mice the NPY-positive fiber plexus in the molecular layer (m) and in stratum lacunosum-moleculare of CA1 (l-m) is darker (arrows), and diffuse NPY-immunoreactivity appears in the hilus and in stratum lucidum of CA3 (arrowheads), where granule cell axons project. The NPY-immunoreactive fiber plexus in the distal CA3 field is wider in the somatostatin knockout mouse because of a slight difference in the plane of section. Scale bar, 250 μm.

### 3.3. Kindling

Age-matched male, wild type ($n = 11$) and somatostatin knockout mice ($n = 13$) were kindled by daily perforant path stimulation. To assess seizure severity, the average duration of all afterdischarges was calculated for each mouse. Afterdischarge duration tended to be slightly longer in somatostatin knockout mice ($19.9 \pm 0.9$ s) than in controls ($17.6 \pm 0.6$ s, $P < 0.06$, $t$-test; Fig. 7). However, the number of treatments to reach five stage 4–5 seizures was similar in somatostatin knockout mice ($17.9 \pm 1.5$) and controls ($16.6 \pm 2.1$, $P > 0.6$, $t$-test; Fig. 8).

## 4. Discussion

The principal findings of this study are (1) somatostatin knockout mice displayed normal Nissl staining, Timm staining, acetylcholinesterase staining, and immunocytochemistry for NPY, parvalbumin, calbindin, and calretinin in the dentate gyrus, and they had normal numbers of hilar neurons. (2) In response to systemic kainic acid, somatostatin knockout mice tended to have a shorter latency to stage 5 behavioral seizure activity, more severe maximal behavioral seizure scores, and higher mortality than wild type controls. (3) In response to perforant path kindling,

somatostatin knockout mice tended to have slightly longer afterdischarges than controls but kindled at a similar rate. These findings suggest that the dentate gyrus develops normally and does not display obvious compensatory changes in somatostatin knockout mice, and that somatostatin may be mildly anticonvulsant in wild type controls.

In these experiments, no developmental or compensatory changes were detected in somatostatin knockout mice. Acetylcholinesterase staining suggests the dentate gyrus receives a normal projection from the septum. Timm staining suggests that the development of major axon projections from the entorhinal cortex, the ipsilateral associational pathway, and the granule cell axon projections are not disrupted. Calbindin, calretinin, and parvalbumin-immunocytochemistry suggests that other interneurons of the dentate gyrus develop normally. Somatostatin knockout mice have normal numbers of hilar neurons, suggesting that hilar interneurons that normally would express somatostatin are not lost during development, despite their lack of somatostatin. NPY is expressed in many somatostatinergic neurons in the dentate gyrus (Chan-Palay, 1987; Köhler et al., 1987; Deller and Leranth, 1990), it has anticonvulsant effects (Woldbye et al., 1996, 1997; Klapstein and

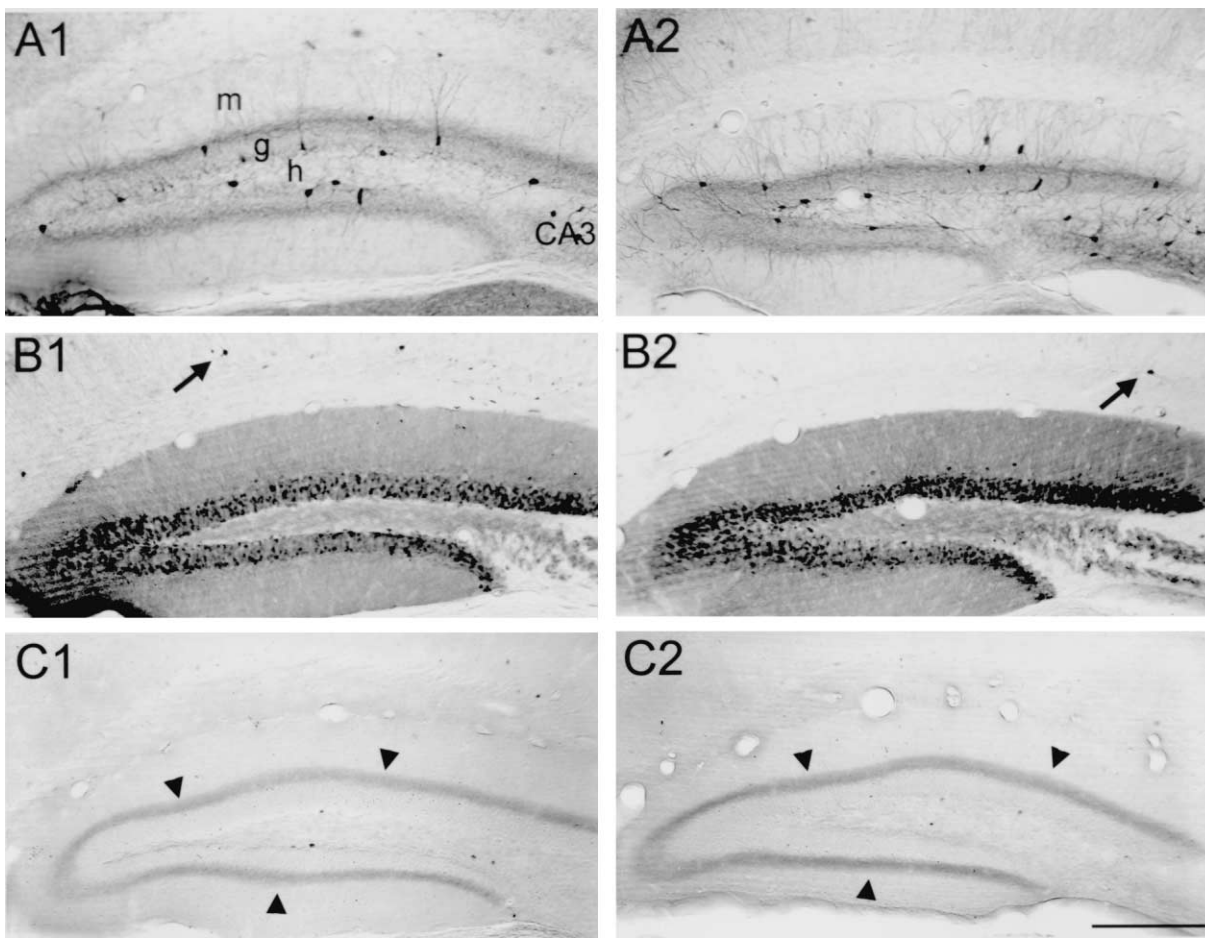


Fig. 4. Similar parvalbumin-, calbindin-, and calretinin-immunoreactivity in the dentate gyrus of wild type (1) and somatostatin knockout mice (2). (A) Parvalbumin-positive somata are evident in or near the granule cell layer (g). (B) Granule cells and interneurons, especially in CA1 (arrows), are calbindin-positive. (C) Some somata in the hilus (h) and a fiber plexus in the inner molecular layer (m; arrow heads) are calretinin-positive. CA3 = CA3 pyramidal cell layer. Scale bar, 250 μm.

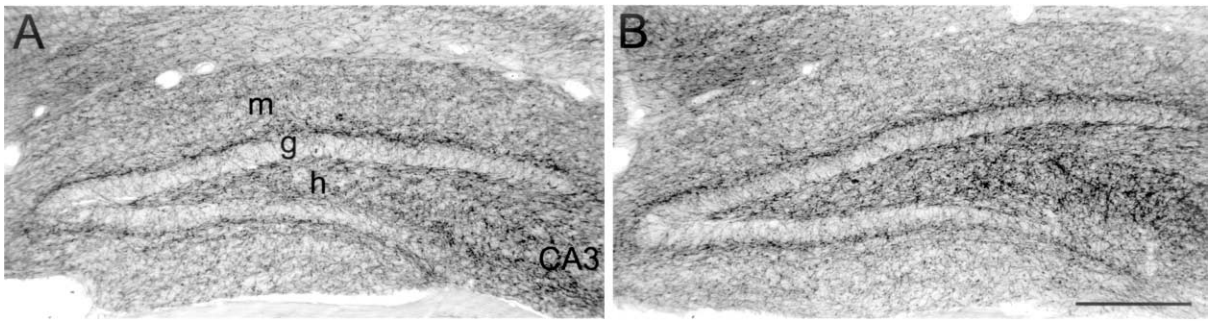


Fig. 5. Similar acetylcholinesterase histochemistry in the dentate gyrus of wild type (A) and somatostatin knockout mice (B). The densest fiber staining in both mice is in the inner molecular layer. h, Hilus; g, granule cell layer; m, molecular layer; CA3 = CA3 pyramidal cell layer. Scale bar, 250 μm.

Colmers, 1997), and its expression is upregulated by seizure activity (de Lanerolle et al., 1989; Sloviter, 1989; Gruber et al., 1994; Kragh et al., 1994; Tønder et al., 1994; Schwarzer et al., 1995). NPY knockout mice are clearly more susceptible to seizure activity (Baraban et al., 1997). Therefore, increased NPY expression might compensate for the loss of somatostatin in knockout mice. However, compared with wild type mice, there was no obvious difference in NPY-staining in somatostatin knockout mice before or after kindling. In summary, although we cannot exclude the possibility of undetected developmental abnormalities or compensatory mechanisms in somatostatin knockout mice, none were evident.

Our findings of slightly heightened seizure severity in somatostatin knockout mice are consistent with previous studies that suggest that somatostatin has anticonvulsant effects. The hypothesis of de Lanerolle et al. (1989) predicts that loss of hilar somatostatinergic interneurons reduces functional inhibition of dentate granule cells. At least four different somatostatin receptor subtypes ($sst_1$–$sst_4$) are expressed in the dentate gyrus (Tran et al., 1985; Krantic et al., 1990; Thoss et al., 1995). The electrophysiological effects of somatostatin on hippocampal neurons have been studied most extensively in the CA1 field. Somatostatin inhibits CA1 pyramidal cells (Watson and Pittman, 1988; but see Scharfman and Schwartzkroin, 1988) by augmenting at least one potassium conductance (M-current; Moore et al., 1988) and blocking the N-type high-voltage-activated calcium conductance (Ishibashi and Akaike, 1995). Somatostatin depresses excitatory, but not inhibitory, neurotransmission in CA1 (Tallent and Siggins, 1997; but see Scharfman and Schwartzkroin, 1989) by blocking the release of glutamate from presynaptic terminals (Boehm and Betz, 1997). The effects of somatostatin on granule cells are unknown, but the loss of hilar somatostatinergic interneurons might result in the loss of inhibitory effects in the dentate gyrus, like that seen in CA1. Somatostatin reduces epileptiform activity in CA1 and CA3 in vitro (Tallent and Siggins, 1999), and a somatostatin analog injected into the dentate gyrus blocks kainate-in-

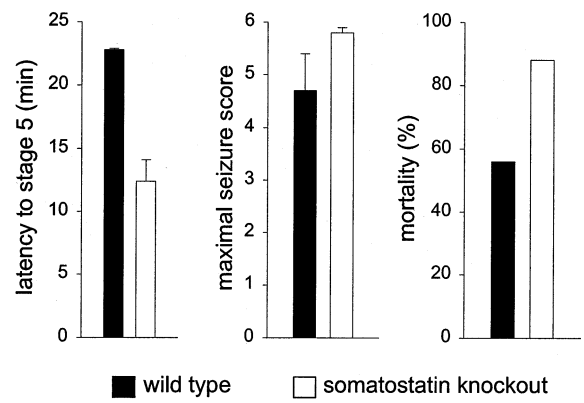


Fig. 6. Kainate-induced seizures in wild type ($n = 16$) and somatostatin knockout mice ($n = 9$). Somatostatin knockout mice tend to have a shorter average latency to stage 5 seizures ($P < 0.07$, $t$-test), a higher average maximal seizure score ($P < 0.05$, $t$-test), and a higher mortality rate than controls ($P < 0.08$, $\chi^2$-test). Error bars represent S.E.M.

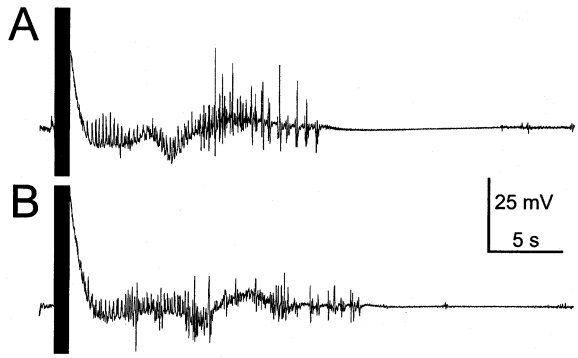


Fig. 7. Afterdischarges recorded in the dentate gyrus of a wild type (A) and somatostatin knockout mouse (B) in response to a perforant path kindling stimulus (1 s train of 1 ms duration pulses at 60 Hz, appears as black vertical band). The average afterdischarge duration of somatostatin knockout mice tends to be slightly longer than that of controls (see text).

duced seizures (Vezzani et al., 1991). Monno et al. (1993) reported that infusion of anti-somatostatin serum into the hippocampus enhances the rate of kindling but does not significantly affect the average or cumulative afterdischarge durations in rats. In contrast, we find no difference in the rate of kindling but slightly longer average afterdischarge duration in somatostatin knockout compared with wild type mice. The different results of the studies may be related to species differences or to differences in the methods used to reduce somatostatin availability.

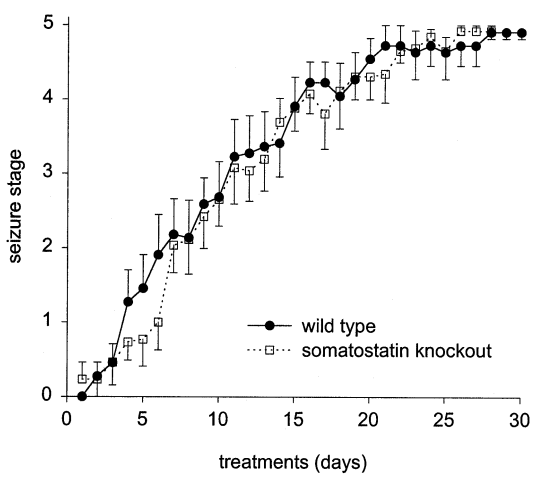


Fig. 8. Kindling rate is similar in wild type ($n = 11$) and somatostatin knockout mice ($n = 13$). Values represent mean, and error bars indicate S.E.M. Kindling stopped after a mouse displayed 5-stage 4 or 5 seizures. In this graph, mice were assigned a score of 5 for the days after kindling was complete.

Our findings suggest that somatostatin may be mildly anticonvulsant, but its loss alone is unlikely to account for seizures in temporal lobe epilepsy. Somatostatin knockout mice do not exhibit spontaneous seizures, their seizure severity is only slightly worse than wild type mice, and they do not kindle faster than wild type mice. Neuropeptide release requires intense stimulation (Hökfelt, 1991; Vilim et al., 1996), and we cannot exclude the possibility that somatostatin was not released sufficiently from hilar interneurons in wild type mice to exert a more dramatic effect that would be more obviously lacking in the knockout mice. However, the methods used in this study—limbic seizures induced by kainate and tetanic stimulation of perforant path fibers—are intense and are likely to activate neurons in the dentate gyrus. Another possible explanation for a lack of more dramatic differences between the wild type and somatostatin knockout mice is their genetic background. C57BL/6J mice are relatively resistant to kainate-induced neurodegeneration (Schauwecker and Steward, 1997). It may be useful to repeat the comparison with mice of a different background stain (e.g. 129).

The loss of somatostatin-immunoreactive hilar interneurons may be important in temporal lobe epileptogenesis, even if the actions of the peptide somatostatin are not the most critical factor. Hilar somatostatin-immunoreactive interneurons are GABAergic (Somogyi et al., 1984; Kosaka et al., 1988; Esclapez and Houser, 1995), therefore, their loss might reduce the tissue's capacity to release GABA. In addition, many somatostatinergic neurons in the dentate gyrus express NPY (Chan-Palay, 1987; Köhler et al., 1987; Deller and Leranth, 1990), which has anticonvulsant effects (Woldbye et al., 1996, 1997; Baraban et al., 1997; Klapstein and Colmers, 1997). Normal expression and release of GABA and NPY by hilar interneurons in somatostatin knockout mice may explain, in part, the lack of a more severe epileptic phenotype.

## Acknowledgements

Supported by the Medical Research Foundation of Oregon (MJL) and NIH/NINDS grants NS01778 and NS39110 (PSB). Paul Buckmaster is a recipient of a Burroughs Wellcome Fund Career Award. We thank K. Carey for assistance with the acetylcholinesterase staining.

## References

Baraban, S.C., Hollopeter, G., Erickson, J.C., Schwartzkroin, P.A., Palmiter, R.D., 1997. Knock-out mice reveal a critical antiepileptic role for neuropeptide Y. J. Neurosci. 17, 8927–8936.

Blasco-Ibáñez, J.M., Freund, T.F., 1997. Distribution, ultrastructure, and connectivity of calretinin-immunoreactive mossy cells of the mouse dentate gyrus. Hippocampus 7, 307–320.

Boehm, S., Betz, H., 1997. Somatostatin inhibits excitatory transmission in rat hippocampal synapses via presynaptic receptors. J. Neurosci. 17, 4066–4075.

Buckmaster, P.S., Dudek, F.E., 1997. Neuron loss, granule cell axon reorganization, and functional changes in the dentate gyrus of epileptic kainate-treated rats. J. Comp. Neurol. 385, 385–404.

Buckmaster, P.S., Jongen-Rêlo, A.L., 1999. Highly specific neuron loss preserves lateral inhibitory circuits in the dentate gyrus of kainate-induced epileptic rats. J. Neurosci. 19, 9519–9529.

Buckmaster, P.S., Kunkel, D.D., Robbins, R.J., Schwartzkroin, P.A., 1994. Somatostatin-immunoreactivity in the hippocampus of mouse, rat, guinea pig and rabbit. Hippocampus 4, 167–180.

Chan-Palay, V., 1987. Somatostatin immunoreactive neurons in the human hippocampus and cortex shown by immunogold/silver intensification on vibratome sections; coexistence with neuropeptide Y, and effects of Alzheimer-type dementia. J. Comp. Neurol. 260, 201–223.

de Lanerolle, N.C., Kim, J.H., Robbins, R.J., Spencer, D.D., 1989. Hippocampal interneuron loss and plasticity in human temporal lobe epilepsy. Brain Res. 495, 387–395.

Deller, T., Leranth, C., 1990. Synaptic connections of neuropeptide Y (NPY) immunoreactive neurons in the hilar area of the rat hippocampus. J. Comp. Neurol. 300, 433–447.

Engel, J. Jr, Williamson, P.D., Wieser, H.-G., 1997. Mesial temporal lobe epilepsy. In: Engel, J. Jr, Pedley, T.A. (Eds.), Epilepsy: A Comprehensive Textbook. Lippincott-Raven, Philadelphia, PA, pp. 2417–2426.

Esclapez, M., Houser, C.R., 1995. Somatostatin neurons are a subpopulation of GABA neurons in the rat dentate gyrus: evidence from colocalization of pre-prosomatostatin and glutamate decarboxylase messenger RNAs. Neuroscience 64, 339–355.

Freund, T.F., Ylinen, A., Miettinen, R., Pitkänen, A., Lahtinen, H., Baimbridge, K.G., Riekkinen, P.J., 1991. Pattern of neuronal death in the rat hippocampus after status epilepticus. Relationship to calcium binding protein content and ischemic vulnerability. Brain Res. Bull. 28, 27–38.

Fujise, N., Liu, Y., Hori, N., Kosaka, T., 1997. Distribution of calretinin immunoreactivity in the mouse dentate gyrus: II. Mossy cells, with special reference to their dorsoventral difference in calretinin immunoreactivity. Neuroscience 82, 181–200.

Gruber, B., Gerber, S., Rupp, E., Sperk, G., 1994. Differential NPY mRNA expression in granule cells and interneurons of the rat dentate gyrus after kainic acid injection. Hippocampus 4, 474–482.

Havlicek, V., Friesen, H.G., 1979. Comparison of behavioral effects of somatostatin and β-endorphin in animals. In: Collu, R. (Ed.), Central Nervous System Effects of Hypothalamic Hormones and Other Peptides. Raven, New York, pp. 381–402.

Higuchi, T., Sickand, G.S., Kato, N., Wada, J.A., Friesen, H.G., 1983. Profound suppression of kindled seizures by cysteamine: possible role of somatostatin to kindled seizures. Brain Res. 288, 359–362.

Hökfelt, T., 1991. Neuropeptides in perspective: the last 10 years. Neuron 7, 867–879.

Houser, C.R., Esclapez, M., 1996. Vulnerability and plasticity of the GABA system in the pilocarpine model of spontaneous recurrent seizures. Epilep. Res. 26, 207–218.

Ishibashi, H., Akaike, N., 1995. Somatostatin modulates high-voltage-activated $Ca^{2+}$ channels in freshly dissociated rat hippocampal neurons. J. Neurophysiol. 74, 1028–1036.

Johansen, F.F., Zimmer, J., Diemer, N.H., 1987. Early loss of somatostatin neurons in dentate hilus after cerebral ischemia in the rat precedes CA-1 pyramidal cell loss. Acta Neuropathol. (Berlin) 73, 110–114.

Klapstein, G.J., Colmers, W.F., 1997. Neuropeptide Y suppresses epileptiform activity in rat hippocampus in vitro. J. Neurophysiol. 78, 1651–1661.

Köhler, C., Ericksson, L.G., Davies, S., Chan-Palay, V., 1987. Co-localization of neuropeptide tyrosine and somatostatin immunoreactivity in neurons of individual subfields of the rat hippocampal region. Neurosci. Lett. 78, 1–6.

Kosaka, T., Wu, J.-Y., Benoit, R., 1988. GABAergic neurons containing somatostatin-like immunoreactivity in the rat hippocampus and dentate gyrus. Exp. Brain Res. 71, 388–398.

Kragh, J., Tønder, N., Finsen, B.R., Zimmer, J., Bolwig, T.G., 1994. Repeated electroconvulsive shocks cause transient changes in rat hippocampal somatostatin and neuropeptide Y immunoreactivity and mRNA in situ hybridization signals. Exp. Brain Res. 98, 305–313.

Krantic, S., Martel, J.-C., Weissmann, D., Pujol, J.-F., Quirion, R., 1990. Quantitative radiographic study of somatostatin receptor heterogeneity in the rat extrahypothalamic brain. Neuroscience 39, 127–137.

Liu, Y., Fujise, N., Kosaka, T., 1996. Distribution of calretinin immunoreactivity in the mouse dentate gyrus. I. General description. Exp. Brain Res. 108, 389–403.

Liu, H., Cao, Y., Basbaum, A.I., Mazarati, A.M., Sankar, R., Wasterlain, C.G., 1999. Resistance to excitotoxin-induced seizures and neuronal death in mice lacking the preprotachykinin A gene. Proc. Natl. Acad. Sci. USA 96, 12096–12101.

Lothman, E.W., Collins, R.C., 1981. Kainic acid induced limbic seizures: metabolic, behavioral, electroencephalographic and neuropathological correlates. Brain Res. 218, 299–318.

Low, M.J., Otero Corchón, V., Parlow, A.F., Ramirez, J.L., Kumar, U., Patel, Y.C., Rubinstein, M., 2001. Somatostatin is required for masculinization of growth hormone-regulated hepatic gene expression but not of somatic growth. J. Clin. Invest. 12, 1571–1580.

Lowenstein, D.H., Thomas, M.J., Smith, D.H., McIntosh, T.K., 1992. Selective vulnerability of dentate hilar neurons following traumatic brain injury: a potential mechanistic link between head trauma and disorders of the hippocampus. J. Neurosci. 12, 4846–4853.

Magloczky, Z., Freund, T.F., 1993. Selective neuronal death in the contralateral hippocampus following unilateral kainate injections into the CA3 subfield. Neuroscience 56, 317–336.

Mathern, G.W., Babb, T.L., Pretorius, J.K., Leite, J.P., 1995. Reactive synaptogenesis and neuron densities for neuropeptide Y, somatostatin, and glutamate decarboxylase immunoreactivity in the epileptogenic human fascia dentata. J. Neurosci. 15, 3990–4004.

Mitchell, J., Gatherer, M., Sundstrom, L.E., 1995. Loss of hilar somatostatin neurons following tetanus toxin-induced seizures. Acta Neuropathol. 89, 425–430.

Monno, A., Rizzi, M., Samanin, R., Vezzani, A., 1993. Anti-somatostatin antibody enhances the rate of hippocampal kindling in rats. Brain Res. 602, 148–152.

Moore, S.D., Madamba, S.G., Joels, M., Siggins, G.R., 1988. Somatostatin augments the M-current in hippocampal neurons. Science 239, 278–280.

Morrison, R.S., Wenzel, H.J., Kinoshita, Y., Robbins, C.A., Donehower, L.A., Schwartzkroin, P.A., 1996. Loss of the p53 tumor suppressor gene protects neurons from kainate-induced cell death. J. Neurosci. 16, 1337–1345.

Nadler, J.V., 1981. Kainic acid as a tool for the study of temporal lobe epilepsy. Life Sci. 29, 2031–2042.

Racine, R.J., 1972. Modification of seizure activity by electrical stimulation: II. Motor seizures. Electroenceph. Clin. Neurophysiol. 32, 281–294.

Robbins, R.J., Brines, M.L., Kim, J.H., Adrian, T., de Lanerolle, N., Welsh, S., Spencer, D.D., 1991. A selective loss of somatostatin in the hippocampus of patients with temporal lobe epilepsy. Ann. Neurol. 29, 325–332.

Rubinstein, M., Goodman, R.H., Low, M.J., 1992. Targeted expression of somatostatin in vasopressinergic magnocellular hypothalamic neurons of transgenic mice. Mol. Cell. Neurosci. 3, 152–161.

Scharfman, H.E., Schwartzkroin, P.A., 1988. Further studies of the effect of somatostatin and related peptides in area CA1 of rabbit hippocampus. Cell. Mol. Neurobiol. 8, 411–429.

Scharfman, H.E., Schwartzkroin, P.A., 1989. Selective depression of GABA-mediated IPSPs by somatostatin in area CA1 of rabbit hippocampal slices. Brain Res. 493, 205–211.

Schauwecker, P.E., Steward, O., 1997. Genetic determinants of susceptibility to excitotoxic cell death: implications for gene targeting approaches. Proc. Natl. Acad. Sci. USA 94, 4103–4108.

Schwarzer, C., Williamson, J.M., Lothman, E.W., Vezzani, A., Sperk, G., 1995. Somatostatin, neuropeptide Y, neurokinin B and cholecystokinin immunoreactivity in two chronic models of temporal lobe epilepsy. Neuroscience 69, 831–845.

Sloviter, R.S., 1987. Decreased hippocampal inhibition and a selective loss of interneurons in experimental epilepsy. Science 235, 73–76.

Sloviter, R.S., 1989. Chemically defined hippocampal interneurons and their possible relationship to seizure mechanisms. In: Chan-Palay, V., Köhler, C. (Eds.), The Hippocampus—New Vistas. Academic Press, New York, pp. 443–461.

Somogyi, P., Hodgson, A.J., Smith, A.D., Nunzi, M.G., Gorio, A., Wu, J.-Y., 1984. Different populations of GABAergic neurons in the visual cortex and hippocampus of cat contain somatostatin- or cholecystokinin-immunoreactive material. J. Neurosci. 4, 2590–2630.

Sperk, G., 1994. Kainic acid seizures in the rat. Prog. Neurobiol. 42, 1–32.

Sperk, G., Marksteiner, J., Bruber, B., Bellmann, R., Mahata, M., Ortler, M., 1992. Functional changes in neuropeptide Y- and somatostatin-containing neurons induced by limbic seizures in the rat. Neuroscience 50, 831–846.

Tallent, M.K., Siggins, G.R., 1997. Somatostatin depresses excitatory but not inhibitory neurotransmission in rat CA1 hippocampus. J. Neurophysiol. 78, 3008–3018.

Tallent, M.K., Siggins, G.R., 1999. Somatostatin acts in CA1 and CA3 to reduce hippocampal epileptiform activity. J. Neurophysiol. 81, 1626–1635.

Thoss, V.S., Perez, J., Duc, D., Hoyer, D., 1995. Embryonic and postnatal mRNA distribution of five somatostatin receptor subtypes in the rat brain. Neuropharmacology 34, 1673–1688.

Tønder, N., Kragh, J., Finsen, B.R., Bolwig, T.G., Zimmer, J., 1994. Kindling induces transient changes in neuronal expression of somatostatin, neuropeptide Y and calbindin in adult rat hippocampus and fascia dentata. Epilepsia 35, 1299–1308.

Tran, V.T., Beal, M.F., Martin, J.B., 1985. Two types of somatostatin receptors differentiated by cyclic analogs. Science 228, 492–495.

Vezzani, A., Serafini, R., Stasi, M.A., Viganò, G., Rizzi, M., Saminin, R., 1991. A peptidase-resistant cyclic octapeptide analogue of somatostatin (SMS 201-995) modulates seizures induced by quinolinic and kainic acid differently in the rat hippocampus. Neuropharmacology 30, 345–352.

Vilim, F.S., Cropper, E.C., Price, D.A., Kupfermann, I., Weiss, K.R., 1996. Release of peptide cotransmitters in Aplysia: regulation and functional consequences. J. Neurosci. 16, 8105–8114.

Watson, T.W.J., Pittman, Q.J., 1988. Somatostatin (14) and (28) but not somatostatin (1–12) hyperpolarize CA1 pyramidal neurons in vitro. Brain Res. 448, 40–45.

West, M.J., Slomianka, L., Gundersen, H.J.G., 1991. Unbiased stereological estimation of the total number of neurons in the subdivisions of the rat hippocampus using the optical fractionator. Anat. Rec. 231, 482–497.

Woldbye, D.P.D., Madsen, T.M., Larsen, P.J., Mikkelsen, J.D., Bolwig, T.G., 1996. Neuropeptide Y inhibits hippocampal seizures and wet dog shakes. Brain Res. 737, 162–168.

Woldbye, D.P.D., Larsen, P.J., Mikkelsen, J.D., Klemp, K., Madsen, T.M., Bolwig, T.G., 1997. Powerful inhibition of kainic acid seizures by neuropeptide Y via Y5-like receptors. Nat. Med. 3, 761–764.